Journal of Electronic Materials, Vol. 3, No. 2, 1974

EFFECTS OF HCl AND Cl_2 ADDITIONS ON SILICON OXIDATION KINETICS

Y. J. van der Meulen and J. G. Cahill

IBM Thomas J. Watson Research Center
Yorktown Heights, New York 10598

(Received September 28, 1973; revised December 7, 1973)

The growth kinetics of SiO_2 films (100-18000Å) on [100], 2Ωcm silicon have been investigated between 900-1100°C with additions of 0-9 vol.% HCl or 0-2 vol.% Cl_2 to the dry oxygen ambient. The thickness-time data could best be fitted numerically to a mixed linear-parabolic equation that included a correction for fast initial growth. Equivalent amounts of chlorine (e.g., 2 vol.% HCl or 1 vol.% Cl_2) produced completely different effects on the rate of SiO_2 growth. The quantitative effects of halogen additions were studied in greatest detail at 900°C. At that temperature, the parabolic rate constant increased linearly with the HCl concentration. At the same time, the linear rate constant remained constant. Both rate constants did change when Cl_2 was used as an additive. The effect of HCl additions on the parabolic rate constant reaches a maximum around 1000°C. Possible mechanisms for the halogen effects are discussed, and it is seen that the gas phase reaction $4\ HCl + O_2 \rightarrow 2\ H_2O + 2\ Cl_2$ is not reflected in the growth kinetics.

Key words: silicon oxidation, silicon dioxide, HCl, Cl_2.

Introduction

In recent years several studies have reported on the beneficial effects of adding small amounts (0-10 vol.%) of chlorine containing species to the dry oxygen ambient during the thermal oxidation of silicon wafers. Such additions of HCl or Cl_2 result in enhanced minority carrier lifetime in the silicon substrate (1, 2), as well as in improved electrical characteristics of the silicon dioxide when subjected to high electric fields (3,4). The first effect is generally thought to be due to the gettering and subsequent removal as gaseous halides of a number of heavy metal impurities, which would otherwise create states near the center of the silicon band gap and thus serve as recombination centers. The second effect stems from the entrapment and neutralization of contaminant sodium ions in the oxide close to the silicon surface, presumably as a result of the earlier incorporation of chlorine in the same region. Furthermore, the use of such additives during so-called wet oxidation (i.e., oxidation done in steam or in water-saturated oxygen) does not result in similar beneficial effects in either the substrate or the oxide (1, 5).

Incorporation of chlorine into SiO_2 grown under addition of HCl or Cl_2 takes place (5, 6, 7), and small changes of the oxide refractive index have also been measured (7). Although the overall SiO_2 growth rate as reported by Kriegler et al is quite strongly enhanced by halogens, no kinetic data have been published thus far as a function of temperature, additive, or concentration. The present study documents the changes in the oxidation kinetics in greater detail. It will be seen that such effects show a particular dependence on the additive, i.e., the formation of oxides in O_2 + HCl ("HCl oxides"), follows quite different kinetics than that of oxides grown in O_2 + Cl_2 ("Cl_2 oxides").

Experimental Procedures

Chem-mechanically polished silicon wafers ([100]-oriented, 1 1/4 in. diam., p-type, 2 Ωcm) were used in this investigation. Cleaning, oxide growth and ellipsometric thickness evaluation were all performed as described earlier (8). To obtain sufficient accuracy, single exper-

iments were generally performed with three wafers at a time. The commercial HCl and Cl_2 gases used were of 99.99+% purity and no further purification was attempted. Mixing of oxygen and additive took place just before the gas entered the double-walled, fused silica furnace tube. Monel pressure regulators and teflon tubing were used to handle the corrosive gases. When working at oxidation temperatures of 1000°C and higher, more uniform oxides could be grown by inserting the wafers directly into the oxidizing ambient than by warming them up in nitrogen (8).

The conditions under which the SiO_2 growth rate was determined are listed in Table I. Considerable trouble was encountered growing uniform oxides in O_2 + Cl_2 at temperatures in excess of 1000°C, and no kinetic analysis was performed for Cl_2 oxides at 1100°C. For growth in O_2 + HCl at that temperature, voids were observed underneath thick ($\sim$ 10,000 Å) oxides, and the silicon substrates were visibly etched during such oxidation runs.

Table I - Summary of Experimental Conditions.

T(°C)	Vol % HCl	Vol % Cl_2
900	0, 1, 2, 4.5, 9	0.5
1000	0, 4.5	0.5
1100	0, 4.5	

Data Analysis

In the past, the kinetics of the thermal formation of silicon dioxide on silicon have been studied for both dry and wet oxidation as a function of numerous parameters (substrate orientation, temperature, degree of contamination, partial pressure of oxygen or water vapor, etc.). Under almost all conditions the relation between oxide thickness and time is best represented by a mixed linear-parabolic equation,

$$\frac{d_{ox}^2 - d_o^2}{k_{par}} + \frac{d_{ox} - d_o}{k_{lin}} = t \qquad (1)$$

where d_{ox} is the oxide thickness, d_o a correction, t the oxidation time, and k_{par} and k_{lin} are the parabolic and linear rate constants, respectively. The parameter d_o has been associated with a rapid, initial oxidation mechanism which becomes unimportant as the oxide thickness increases (9). The two rate constants and d_o are functions of the experimental conditions. In the case of oxide formation in oxygen, the first term on the left-hand side of the equation arises from the diffusional limitation of the oxygen transport through the thickening SiO_2 film; the second, linear term arises from the limitation imposed by the reaction to form silicon dioxide at the $Si|SiO_2$ interface. The dependence of k_{lin} on the oxygen partial pressure indicates that more than a single oxygen species participates in the reaction (8). It will be assumed that HCl or Cl_2 additions do not change the basic mechanism of SiO_2 formation. Thus, oxidant species are held responsible for the mass transport through the growing oxide.

For a given temperature and additive concentration, a number (n=6-10) of experimental pairs (t, d_{ox}) were generated, and the variable metric method (10) was then used to calculate the unknown parameters in Eq. (1). The final optimum values were arrived at by minimizing a quantity F defined, by

$$F = \sum_{n} [\{(d_{ox})_{calc.}/(d_{ox})_{meas.}\}-1]^2 \qquad (2)$$

for a given set of (t,d_{ox}) points. It can be seen from this expression that equal relative weight was given to all experimental points.

For shorter oxidation runs the predominant error is caused by uncertainties in the warm-up time, whereas for runs of longer duration, a small offset in the furnace temperature as well as random fluctuations in the additive concentration will introduce some error in the oxide thickness. These random effects cannot be quantized easily and their relative influence can only be judged from the value of F or, even better, from the value of a quantity P

$$P = 100 \times (F/n)^{1/2} \qquad (3)$$

The value of P corresponds quite closely to the average percentual error per experimental point and indicates how well

a given set of data can be fitted to Eq. (1).

Equation (1) contains two measured quantities as well as three parameters that are to be calculated, and we usually generated a large number of oxidation times and corresponding oxide thicknesses. However, regardless of the amount of experimental data under a given set of conditions, the parameters cannot all be determined equally well at all temperatures. This is caused by the fact that the relative contribution of either of the terms on the left-hand side of the equation can become so large as to be completely dominant over much of the thickness-time range studied. The determination of the rate constant contained in the other term is then subject to severe error. Likewise, d_o can only be determined accurately when d_{ox} values of the same order of magnitude are included in the analysis. This is especially true if the first term is dominant over much of the thickness range investigated. Generally speaking, this means that with increasing temperature the accuracy of the analysis is best maintained for k_{par}, but decreases steadily for both k_{lin} and d_o regardless of the other conditions employed. For these reasons, 900°C was chosen as the temperature at which to perform the most complete analysis. It should be realized, however, that analytic measurements were not sufficiently sensitive to confirm the presence of chlorine in oxides grown at that temperature (7), making it impossible to correlate the changes in the kinetic parameters with the amount of chlorine actually incorporated into the oxide.

Gas Phase Equilibria

Another factor that influences the kinetic analysis is the fact that when HCl is used as an additive, the following gas phase equilibrium will be established,

$$4\ HCl + O_2 \overset{\leftarrow}{\rightarrow} 2\ H_2O + 2\ Cl_2 \tag{4}$$

with an equilibrium constant

$$K = \frac{[H_2O]^2\ [Cl_2]^2}{[HCl]^4\ [O_2]} = \frac{\bar{P}_{H_2O}^{\,2} \cdot \bar{P}_{Cl_2}^{\,2}}{\bar{P}_{HCl}^{\,4} \cdot \bar{P}_{O_2}} \tag{5}$$

where the brackets and $\bar{p}$'s denote concentrations and partial pressures, respectively. Since the oxygen partial pressure varied only from 0.9 to 1.0 atm in our experiments, in good approximation,

$$K = \frac{\bar{p}_{H_2O}^{\,2} \cdot \bar{p}_{Cl_2}^{\,2}}{\bar{p}_{HCl}^{\,4}} = \frac{(\frac{1}{2}\,a)^2 \cdot (\frac{1}{2}\,a)^2}{(x - a)^4} \tag{6}$$

where x is the volume fraction HCl originally added, and a the volume fraction converted into H_2O and Cl_2. Values of K(T) can be calculated from published equilibrium constants (11, 12) for the equilibria

$$H_2 + \tfrac{1}{2}\,O_2 \overset{\leftarrow}{\rightarrow} H_2O,\ K_A \tag{7}$$

and,

$$\tfrac{1}{2}\,H_2 + \tfrac{1}{2}\,Cl_2 \overset{\leftarrow}{\rightarrow} HCl,\ K_B \tag{8}$$

Combining Eqs. (6), (7) and (8), one finds

$$K = K_A^{\,2} \,/\, K_B^{\,4} \tag{9}$$

Table II - Equilibrium constants defined in Eqs. (7), (8) and (9) as a function of temperature.

T(°K)	$\frac{10^3}{T}$ (°K^{-1})	log K_A	log K_B	log K
298	3.36	40.05	16.67	13.42
400	2.50	29.23	12.59	8.10
600	1.67	18.63	8.52	3.18
800	1.25	13.29	6.49	0.62
1000	1.000	10.06	5.26	-0.92
1200	.825	7.90	4.44	-1.96
1400	.714	6.35	3.84	-2.66

Results for K(T) are listed in Table II. From Eq. (6) one derives the following relations,

$$\bar{P}_{H_2O} = \bar{P}_{Cl_2} = \left\{ \frac{K^{1/4}}{1 + 2K^{1/4}} \right\} x \tag{10}$$

$$\bar{P}_{HCl} = \left\{ \frac{1}{1 + 2K^{1/4}} \right\} x \tag{11}$$

$$\bar{P}_{HCl} / \bar{P}_{Cl_2} = K^{-1/4} \tag{12}$$

The proportionality constants and their ratio have been plotted as a function of temperature in Fig. 1. It can be seen that the HCl/Cl_2 ratio varies almost linearly as a function of temperature between 700°C and 1100°C, and equals 3 at 900°C.

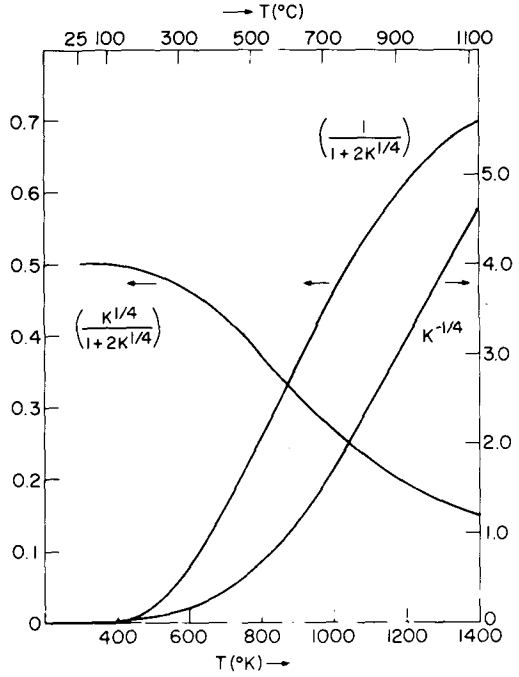

Fig. 1. Constants defined in Eqs. (10)-(12), as a function of temperature.

When Cl_2 is used as an additive, no reaction with the oxygen should occur; however, traces of water vapor present in the gases will influence that situation in a somewhat unpredictable manner. Comparable amounts of water vapor have no significant effect on the equilibrium in the O_2 + HCl case. Note that the calculated equilibrium applies to the gas phase and that no numerical data exist to calculate the equilibria in the solid SiO_2 phase.

Finally, one can calculate (13) that between 800°C and 1100°C the equilibrium pressure of atomic oxygen is less than 10^{-6} atm. The atomic chlorine pressure in the same temperature interval will be less than 10^{-5} atm. for additions of up to 3 vol.% Cl_2 or 9 vol.% HCl. However, the equilibria might be different again in the solid phase.

Results and Discussion

Effect of halogen additions at 900°C

As stated earlier, the largest amount of data was collected at 900°C. Typical growth curves for HCl oxides at that temperature are shown in Figs. 2 and 3 (For greater clarity the data for O_2 + 2% HCl were omitted from these graphs.). The results in the first figure are in the region

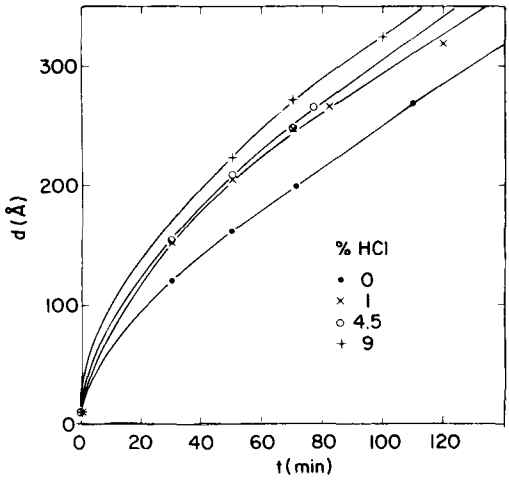

Fig. 2. SiO_2 thickness vs. oxidation time (900°C, short times).

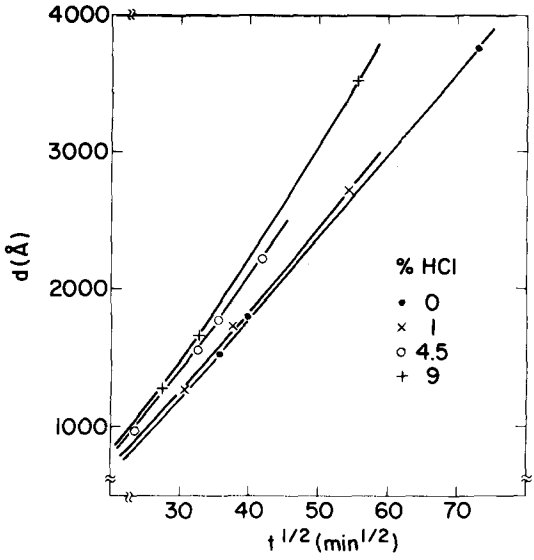

Fig. 3. SiO_2 thickness vs. oxidation time (900°C, long times).

where growth is mainly reaction-rate limited, while the data in Fig. 3 strongly reflect the diffusion-controlled range. Results of the numerical analysis using Eq. (1) are given in the top section of Table III together with results for O_2 + 0.5 vol.%Cl_2. Also listed are the number of experimental points n, and the quantity P defined in Eq. (3). It is seen that this procedure was quite successful with the best agreement found for oxidation in O_2. This is reasonable as it was sometimes difficult to keep the additive concentration sufficiently constant. In the Cl_2-oxide case, deviations occurring from wafer to wafer could be due to traces of water vapor, the concentration of which should vary along the boat holding the wafers, tending to become lower in the downstream direction of the furnace tube. The increased scatter between experiments is reflected in a higher value of P for Cl_2 oxides (cf. Table III) and probably results from small variations in the additive concentration (flow rate). The Cl_2 oxides should be more sensitive towards such fluctuations than the HCl oxides, as an equal concentration of additive causes a far larger effect in the first case. The values used for data fitting were normally obtained by averaging the thicknesses measured on three wafers used in the

same experiment. Fitting Eq. (1) to the minimum and the maximum thickness values measured for O_2 + 0.5% Cl_2 shifted k_{par} by only 9% and hardly affected k_{lin} and d_o.

Table III - Kinetic parameters at 900°C as a function of additive concentration (vol.%). Note, that where d_o = 0, the analysis was done for the linear-parabolic model.

Oxidant	k_{par} ($Å^2$/min)	k_{lin} (Å/min)	d_o (Å)	n	P (%/pt.)
O_2	3940	2.20	64	6	0.48
O_2 + 1% HCl	4275	2.13	114	6	0.95
2	5490	2.21	111	6	1.03
4.5	6420	2.17	114	7	0.75
9	8400	2.11	137	7	0.96
O_2 + 0.5% Cl_2	1846	3.1	175	7	1.32
O_2	3021	3.51	0	7	4.99
O_2 + 9% HCl	4002	4.39	0	7	7.68
O_2 + 0.5% Cl_2	1335	24.6	0	7	3.91

Note that d_o is treated simply as an overall correction as at this time no complete physical or mathematical description exists of the underlying process (9). Thus, it was necessary to exclude from the numerical analysis those datapoints for which this process has not yet reached its completion (e.g., 30 min. in 1% and 4.5% HCl). The decision on when to exclude a specific point was sometimes based on the fact whether such an exclusion would significantly lower the value of P, and had some minor influence on the parameters calculated. Generally, thicknesses up to 2 x d_o were excluded.

To illustrate that 900°C is indeed a very suitable temperature to measure k_{par}, k_{lin} and d_o simultaneously, the relative contributions of the first and second terms

in Eq. (1) to the total oxidation time were calculated using the results for the 100% oxygen case (Table IV). It can be seen that the linear and parabolic processes each are clearly dominant over part of the thickness range, making it possible to calculate both k_{lin} and k_{par} quite accurately. The early dominance of the first, parabolic term in Eq. (1) makes it considerably more difficult to determine k_{lin} at higher temperatures. Such limitations should be kept firmly in mind when evaluating high temperature data, especially when the oxidation model does not take into account all complexities of the total oxidation process. On the other hand, the determination of k_{par} at lower temperatures requires oxidation experiments of much longer duration and carries with it correspondingly greater uncertainty because of possible variations in the additive concentration.

The numerical results obtained for the rate constants depend strongly on the physical model used. This can best be demonstrated using a model in which d_o equals zero, i.e., a purely linear-parabolic model. Three examples of the results of such an analysis are also given in the bottom of Table III. It is seen that the values calculated for k_{par} and k_{lin} differ strongly from the earlier ones.

Table IV - Fractional contributions of the parabolic and linear processes to the total oxidation time (900°C, 100% O_2).

d_{ox} (Å)	$\frac{d_{ox}^2 - 64^2}{3940 \times t}$	$\frac{d_{ox} - 64}{2.20 \times t}$
100	.08	.92
200	.13	.87
500	.24	.76
1000	.37	.63
2000	.54	.46
4000	.69	.31

At the same time the quality of the fit (as indicated by the parameter P) has deteriorated sharply, indicating that this model is less realistic and should therefore be rejected. (The fit becomes even worse when in the purely linear-parabolic case points at lower thicknesses are included.)

From the results in Table III one concludes that k_{lin} is independent of the HCl concentration, and that k_{par} increases almost linearly with additive concentration (Fig. 4). Such a trend in k_{par} can of course not continue indefinitely at higher HCl concentrations. For Cl_2 oxides the results are quite different and show a strong decrease in k_{par} together with higher values for k_{lin} and d_o.

These results can best be discussed further in the context of the differences between oxidations in O_2 + HCl and O_2 + Cl_2. In doing so one has to remember that the O_2 + HCl mixture reacts according to Eq. (4) and produces H_2O and Cl_2 in significant quantities (Table V).

In order to gage the effect of Cl_2 during growth of HCl oxides, a limited comparison is possible with the Cl_2 oxides, i.e., one can probably compare the linear but not the parabolic rate constants. The linear rate constant

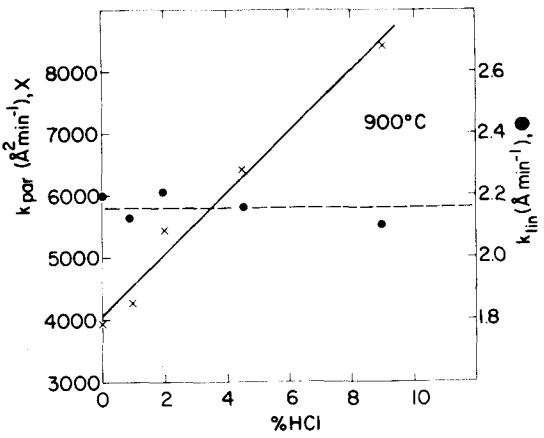

Fig. 4. Parabolic and linear rate constants vs. added HCl concentration.

Table V - Percentual composition of oxidizing ambient at 900°C as a function of starting composition.

Starting Mixture		Oxidizing Ambient			
O_2	HCl	O_2	HCl	H_2O	Cl_2
100	---	100	---	---	---
99	1	99	0.6	0.2	0.2
98	2	98	1.2	0.4	0.4
95.5	4.5	95.5	2.7	0.9	0.9
91	9	09.9	5.5	1.8	1.8

gives an indication of the species participating in the reaction by which SiO_2 is formed at the Si-SiO_2 interface. The addition of 0.5% Cl_2 substantially increased k_{lin} (Table III). However, even for a 9% HCl addition, which should produce approximately 2% Cl_2 in the gas phase, no significant change was measured in k_{lin}. Hence, HCl additions do not appear to result in a substantial, measurable presence of Cl_2 at the inner interface. The parabolic rate constants cannot be used for such a comparison, as they reflect the solubility and diffusivity of not only O_2 but also H_2O (or OH^-) during the growth of HCl oxides, and may be influenced by the difference in chlorine concentration incorporated into these oxides.

As far as H_2O is concerned, somewhat different considerations apply: The linear oxidation rate of [100]-oriented silicon at 900°C in steam at atmospheric pressure is 133Å/min (14), but some uncertainty exists over its pressure dependence, which may be sublinear (9, 14). However, for a linear dependence it follows that the 1.8% H_2O resulting from the addition of 9% HCl could roughly double k_{lin} from its value (2.20 Å/min) in 100% O_2. The available evidence listed in Table III does not show such an effect. In fact, by estimating the possible error in k_{lin} to be approximately 5%, it is calculated that the amount of H_2O present in the SiO_2 at the interface would correspond to no more than 0.1% in the gas phase. As far

as the parabolic rate constant concerns, it is easily verified (using Fick's first law) that if two species participate in a parabolic process, the rate constants can be added to yield an overall value. Thus in our case one can try to ascribe the increase in the parabolic rate constant to the presence of water. At 900°C in steam at atmospheric pressure k_{par} equals 37 x 10^4 $Å^2$/min (14) and is linear with the oxygen pressure (14, 15) making it almost certain that H_2O is the diffusing species. The presence of 1.8% H_2O in the oxidant should increase k_{par} by 6660 $Å^2$/min as compared with a measured increase of 4460 $Å^2$/min. Analogously to the conclusions about chlorine in the preceding paragraph, it can therefore be stated that the water vapor generated by the reaction between O_2 and HCl does not seem to influence the oxidation process as expected.

From the above discussion it is concluded that the reaction between O_2 and HCl (Eq. 4) proceeds considerably further towards Cl_2 and H_2O in the gas phase than in the SiO_2 solid phase. This conclusion can also be drawn from the following experimental observation: When a double-walled furnace tube was used for oxidations in O_2 after being used in O_2 + Cl_2, large upward deviations (up to 75%) from the expected SiO_2 thickness as well as a large spread in thickness among oxides grown in a single experiment were found. These effects persisted for many days, disappearing only very slowly; they were thought to be caused by small amounts of chlorine slowly being leached out of the vitreous silica tube wall. When analogous oxidations were done after use of a tube in O_2 + HCl, the effects were much less and lasted far shorter. This indicates that O_2 + HCl mixtures, although containing similar percentages of chlorine in the gas phase are less apt to dissolve this chlorine in the vitreous silica tube wall than O_2 + Cl_2 mixtures. This reinforces the conclusion that the equilibrium in the solid phase is shifted towards the O_2 + HCl side as compared with the situation in the gas phase.

Effect of temperature

A comparison between oxidations at three different temperatures can be made from the results listed in Table VI. It should be stressed that at 1100°C fitting of the data to three parameters was very difficult and resulted in a

Table VI - Kinetic parameters as a function of temperature and additive concentration.

Oxidant	T (°C)	k_{par} ($Å^2$/min)	k_{lin} (Å/min)	d_o (Å)	n	P (%/pt.)
O_2	900	3940	2.20	64	6	0.48
	1000	16900	8.05	192	7	1.06
	1100	41400	32.5	330	6	0.6
O_2 + 4.5% HCl	900	6420	2.17	114	7	0.75
	1000	44000	10.2	250	7	0.75
	1100	54000	?	?	6	---
O_2 + 0.5% Cl_2	900	1846	3.1	175	7	1.32
	1000	18000	8.3	240	6	1.34

larger uncertainty in k_{lin} than would be the case for a purely linear-parabolic formula. In other words, many combinations of d_o and k_{lin} are possible that yield comparable values for P. However, omission of d_o or arbitrary assignment of a constant value to this parameter is unrealistic. As we saw before, d_o performs a well-defined function at 900°C, and it can be shown that omission of d_o results in substantially higher values of P at all temperatures. A solution to this problem is of course to postulate a kinetic model for the process causing the fast initial growth, rather than work with the final thickness value caused by this process. This would make it possible to use values over the full range of oxide thickness. However, this solution requires a much larger amount of experimental data taken under extremely well-controlled conditions, e.g., by in situ ellipsometry during oxidation at high temperatures (15). Even then, however, it can be expected that the uncertainties at higher temperatures (> 1050°C) will be substantial, basically because the fast initial process and the linear process occur in the same thickness range and thus cannot be separated easily. On the other hand, the value calculated for k_{par} is very

insensitive to these variations in d_o and k_{lin}, and even omitting d_o only lowers it by 10-15%.

The results in Table VI also show that the enhancement of the parabolic rate constant by HCl additions is largest at 1000°C and becomes markedly lower in an absolute as well as relative sense at 1100°C. The strong enhancement at 1000°C provides us with another opportunity to check on the possible role of water vapor: For oxidation in steam at 1000°C, $k_{par} = 58 \times 10^4$ Å^2/min (14). Thus the presence of 0.8% water in the oxidant should increase k_{par} at most by 4660 Å^2/min, as compared with a measured increase of 27100 Å^2/min. Therefore, at 1000°C, as at 900°C, the increase in k_{par} is not directly related to the amount of water present in the oxidative ambient. The same is true at 1100°C; a calculated maximum increase of 7000 Å^2/min, vs. a measured increase of 12600 Å^2/min. The linear rate constant at 1000°C (Table IV) seems somewhat enhanced by the addition of HCl, the value of d_o is also higher. Addition of Cl_2 to the ambient mainly results

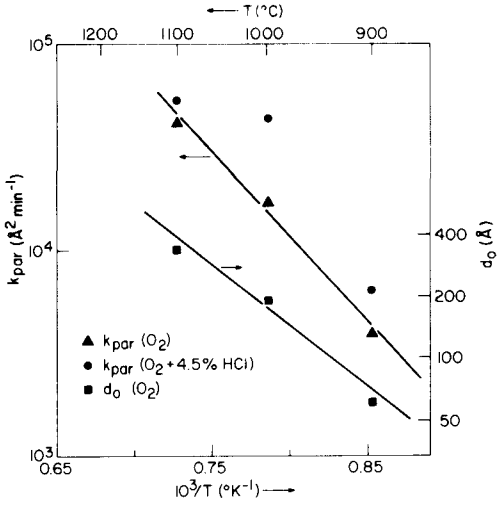

Fig. 5. Kinetic parameters (k_{par}, d_o) as a function of temperature.

in an increased value of d_o at 1000°C.

The values of the parabolic rate constant in oxygen at 1000°C and 1100°C found in this study are quite comparable to values published earlier (9, 16). Due to a lower value at 900°C, the activation energy calculated is somewhat higher (1.64 eV). Similar, recent measurements elsewhere agree with this result (17). The values of k_{par} measured with O_2 + 4.5% HCl as an oxidant can clearly not be described by a single activation energy (Fig. 5). This strongly suggests that the changes occurring in k_{par}, which reflects both the solubility and the diffusivity of oxygen in silicon dioxide, cannot easily exceed a temperature-dependent limit. It is interesting to note that the decrease in oxide refractive index upon addition of HCl to the ambient at 1150°C was also found to be smaller than at 1000°C (7), which supports the concept of a temperature-dependent limit beyond which the structural properties of the oxide are not easily pushed.

Finally, from our data analysis it appears that the value of d_o for oxidation in pure oxygen can be described by an Arrhenius relation with an activation energy of 1.17 eV (Fig. 5). This result is at variance with earlier work (9), in which d_o was found to be temperature-independent. The difference is mainly due to the much lower values of d_o at lower temperatures in the present work [cf. also ref. (8), Fig. 3, indicating $d_o \approx 35$ Å at 850°C].

Summary

Using ellipsometry, the growth kinetics of SiO_2 (100-18000 Å) on [100]-oriented Si wafers have been investigated at various temperatures and ambient concentrations of HCl and Cl_2 in dry O_2. Throughout the range of experimental conditions studied, the linear parabolic model of oxide formation, incorporating a correction for faster initial growth, yields a good fit to the data. Omission of the correction results in a far larger discrepancy between measured and calculated values.

The addition of HCl, which carries with it the formation of water and chlorine in the ambient, enhances the parabolic rate constant at all temperatures. This increase cannot be

related simply to the presence of water or chlorine in the gas; neither can the increased values of the parabolic rate constant be described by a simple Arrhenius type equation. At 900°C, the addition of chlorine to the ambient lowers k_{par} and increases k_{lin} and d_o; at 1000°C, however, the kinetic influence of chlorine is not very pronounced.

It is argued that a more accurate and complete description of the oxidative process is necessary to eliminate uncertainties in d_o and k_{lin} at temperatures above 1000°C. The use of a purely linear-parabolic model may yield better defined results, but is nevertheless not satisfactory because of the discrepancy between theory and experiment.

Acknowledgment

The authors wish to thank J. M. Eldridge for his critical review of the manuscript.

References

1. P. H. Robinson and F. P. Heiman, J. Electrochem. Soc., 118, 141 (1971).

2. R. S. Ronen and P. H. Robinson, J. Electrochem. Soc., 119, 747 (1972).

3. R. J. Kriegler, Y. C. Cheng, and D. R. Colton, J. Electrochem. Soc., 119, 388 (1972).

4. R. J. Kriegler, Appl. Phys. Lett., 20, 449 (1972).

5. R. J. Kriegler, Semiconductor Silicon, p. 363 (The Electrochem. Soc., Princeton, 1973).

6. R. L. Meek, J. Electrochem. Soc., 120, 308 (1973).

7. Y. J. van der Meulen, C. M. Osburn and J. F. Ziegler, J. Electrochem. Soc., 120, 74C (1973).

8. Y. J. van der Meulen, J. Electrochem. Soc., 119, 530 (1972).

9. B. E. Deal and A. S. Grove, J. Appl. Phys., 36, 3770 (1965).

10. R. Fletcher and M. J. Powell, Comp. J., 6, 163 (1963).

11. F. G. Brickwedde, M. Moskow and J. G. Aston, J. Res. Natl. Bur. Stand., 37, 263 (1946).

12. B. J. McBride, S. Heimel, J. G. Ehlers and S. Gordon, NASA-SP-3001 (1963).

13. D. R. Stull and G. C. Sinke, Thermodynamic Properties of the Elements (A.C.S. Monograph, Washington, 1956).

14. W. A. Pliskin, IBM J. Res. Dev., 10, 198 (1966).

15. Y. J. van der Meulen and N. C. Hien, to be published.

16. A. G. Revesz and R. J. Evans, J. Phys. Chem. Solids, 30, 551 (1969).

17. R. Gdula, private communication.